THERMODYNAMIC AND KINETIC STUDIES OF LANTHANIDE(III) COMPLEXES WITH H_5do3ap (1,4,7,10-TETRAAZACYCLODODECANE-1,4,7-TRIACETIC-10-(METHYLPHOSPHONIC ACID)), A MONOPHOSPHONATE ANALOGUE OF H_4dota

Petr TÁBORSKÝ[a1], Přemysl LUBAL[a2,*], Josef HAVEL[a3], Jan KOTEK[b1], Petr HERMANN[b2,*] and Ivan LUKEŠ[b3]

[a] *Department of Analytical Chemistry, Masaryk University, Kotlářská 2, 611 37 Brno, Czech Republic; e-mail: [1] taborak@email.cz, [2] lubal@chemi.muni.cz, [3] havel@chemi.muni.cz*

[b] *Department of Inorganic Chemistry, Charles University, Hlavova 2030, 128 40 Prague 2, Czech Republic; e-mail: [1] modrej@natur.cuni.cz, [2] petrh@natur.cuni.cz, [3] lukes@natur.cuni.cz*

Received July 6, 2005
Accepted September 6, 2005

Solution properties of complexes of a new H_4dota-like ligand containing three acetate and one methylphosphonate pendant arms (H_5do3ap, H_5L) were studied. The ligand exhibits a high last dissociation constant (pK_A = 13.83) as a consequence of the presence of phosphonate moiety. In solution, successive attachment of protons leads to several reorganizations of protonation sites and the neutral zwitterionic species H_5do3ap has the same solution structure as in the solid state, where the nitrogen atom binding methylphosphonate and the opposite nitrogen atoms are protonated. Stability constants with Na^+ and trivalent lanthanide ions (La^{3+}, Ce^{3+}, Eu^{3+}, Gd^{3+}, Lu^{3+}) and Y^{3+} have been determined. The constants are comparable or higher than those of H_4dota due to the higher overall basicity of H_5do3ap. Formation of the stable protonated complexes, as well as complexes with the L:M = 1:2 stoichiometry, was proved. Formation and decomplexation kinetics of the Ce^{3+} and Gd^{3+} complexes were investigated. The mechanism of formation of the H_5do3ap complexes is similar to that observed for H_4dota complexes and the complex species with mono- or diprotonated ligand on the cyclen ring are considered as the reaction intermediates. Acid-assisted decomplexation of H_5do3ap complexes is faster in comparison with those of H_4dota. This is caused by higher basicity of the phosphonate pendant arm and the ring nitrogen atoms, which facilitates the proton transfer from the bulk solution to the nitrogen atoms of cyclen ring.

Keywords: Azacrown compounds; Phosphonate complexes; Macrocyclic ligand; Cyclen derivative; Tetraazacyclododecane; DOTA; Thermodynamics; Kinetics; Crystal structure determination; Potentiometry; Cerium; Gadolinium; Lanthanide cations.

Multidentate ligands and their complexes are frequently used in medicine. Gadolinium(III) complexes of octadentate ligands, having the ninth coordination site occupied with water molecule, are utilized as contrast agents

(CA) in magnetic resonance imaging (MRI)[1]. As doses of such CA containing the toxic metal ion are relatively high, the Gd(III) ion must be encapsulated in stable complexes. Similarly, stable complexes have to be devised for applications of metal radionuclides to diagnosis and therapy in nuclear medicine[2]. The radionuclide complexes are targeted to a diseased tissue by biomolecular vectors, mostly monoclonal antibodies[3] or small peptides[4]. In this case, only a tiny amount of a highly toxic radioisotope is administrated and its complex must survive without any decomplexation in body fluids containing many competing ligands (amino acids, phosphate anion, peptides, etc.) and metal ions (e.g., Ca^{2+}, Zn^{2+}, Cu^{2+}) at much higher concentrations. The ligands, the complexes of which fulfil such stability requirements, are mostly derivatives of two prototype ligands (Chart 1) – acyclic diethylenetriaminepentaacetic acid (H_5dtpa) and macrocyclic 1,4,7,10-tetraazacyclododecane-1,4,7,10-tetraacetic acid (H_4dota).

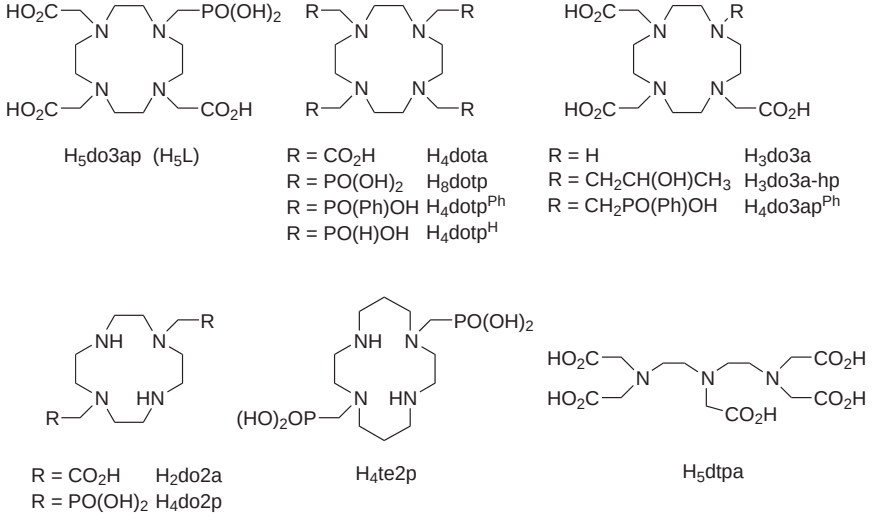

CHART 1

In vivo stability of the complexes may be estimated from thermodynamic and kinetic properties. Thermodynamic stability of metal complexes of H_5dtpa and H_4dota (expressed as stability constants) is very high. However, selectivity (a relative difference between stability constants for various metal ions) is rather low, as all metal ions are complexed with a similar efficiency. Resistance to decomplexation (measured, e.g., as acid-assisted dissociation) is much higher for complexes of the macrocyclic ligands. An additional kinetic property important for the above medicinal utilization is the

rate of complexation. Complexes of the acyclic ligands are formed almost immediately. In solution, the macrocyclic ligands are usually organized in a stable conformation, which blocks an easy entering of the metal ion into the ligand cavity. This leads to a slow complexation, which is often too long to be acceptable for nuclear medicine applications. As properties of the complexes currently approved or investigated for the above utilizations are far from ideal, there is a requirement for designing new ligands whose complexes would be more suitable. Metal complexes of such ligands should exhibit high thermodynamic stability as well as improved selectivity. Kinetic inertness of the complexes should be comparable with that of the macrocyclic ligands and the complexation rate should ideally be similar to that of acyclic ligands.

Such requirements have not been achieved for any class of ligands. Kinetic inertness of complexes of H_5dtpa derivatives was enhanced by introduction of steric hindrance into the diethylenetriamine backbone, e.g., by the replacement of the ethylene chain with the cyclohexane ring[5]. However, ligands based on the polyazamacrocyclic amines are more suitable for further development, as their complexes are inherently thermodynamically stable and kinetically inert[6]. One possibility to change properties of macrocyclic ligands is introduction of methylphosphonate pendant(s) instead of acetic group(s) into polyazapolyacetic acids[7–9]. Fully substituted symmetric phosphonic acid derivatives of tacn (1,4,7-triazacyclononane)[10], cyclen (1,4,7,10-tetraazacyclododecane)[11] or cyclam (1,4,8,11-tetraazacyclotetradecane)[12] form complexes of very high thermodynamic stability and improved selectivity. Kinetic inertness of their lanthanide(III)[13] and copper(II)[14] complexes is sufficient for medicinal use. However, the complexes formed show a high charge, which may limit their usage in medicine. Complexes of tetrakis-(phosphinic acid) derivatives of cyclen exhibit slightly lower thermodynamic stabilities than those of H_4dota, but selectivity, formation kinetics and, in some cases, even kinetic inertness are improved[15–17].

It is well known that tetrasubstituted derivatives of cyclen (e.g., H_4dota) are the most suitable ligands for trivalent lanthanide ions[18]. Therefore, ligands appropriate for lanthanide(III) ions should be based on cyclen skeleton. We have started to study a family of ligands having one acetate group replaced by a phosphonate/phosphinate pendant arm. It was shown that Ln(III) complexes of such ligands with one phosphorus acid pendant arm are very interesting for the design of new MRI CA [19–22]. Solution structure of lanthanide(III) complexes with the monophosphorus acid macrocyclic ligands is very similar to the structure of the corresponding H_4dota complexes – octadentate (4 O + 4 N) coordination of the ligands with one water

molecule coordinated in the apical position[23]. In the gadolinium(III) complexes, the central metal ion exchanges the bound water molecule for the bulk water very fast[19–22] and its residence time is very close to that predicted by theory as an optimal time[1]. In this paper, we report on thermodynamic and kinetic properties of the complexes of H_5do3ap (Chart 1), a monophosphonate derivative of H_4dota.

EXPERIMENTAL

General

Water was purified using a Milli-Q (Millipore) purification system. NMR spectra were recorded on a Varian Unity Plus at 400 MHz for ^{1}H, 169 MHz for ^{31}P{^{1}H} and 100 MHz for ^{13}C{^{1}H} with *t*-BuOH as internal reference (^{1}H and ^{13}C) and 85% H_3PO_4 as external reference (^{31}P). Temperature was controlled by a VT-regulator, containing a thermocouple calibrated using MeOH and $HOCH_2CH_2OH$ according to a literature procedure[24].

Ligand Recrystallization

The ligand H_5do3ap[20a] was recrystallized from water. Its trihydrate (2.50 g) was dissolved in hot water (3 ml) and the solution was left in a closed vial for three weeks. Crystals of H_5do3ap·4H_2O were filtered, washed with EtOH and dried in air overnight. A single crystal suitable for X-ray diffraction studies was selected from the bulk before filtration.

Crystal Structure Determination

The selected crystal of H_5do3ap·4H_2O was mounted on a glass fibre in random orientation using a silicone fat. Diffraction data were collected with graphite-monochromatized MoKα radiation on an Enraf–Nonius KappaCCD diffractometer at 150(1) K (Cryostream Cooler (Oxford Cryosystem)) and analyzed using the HKL DENZO program package[25]. Cell parameters were determined from all data with the same program package[25]. The structure was solved by direct methods, and refined by full-matrix least-squares techniques (SIR92, SHELXL97; refs[26,27]). The scattering factors used for neutral atoms were included in the SHELXL97 program. All non-hydrogen atoms were refined anisotropically; the hydrogen atoms were localized in the difference map of electronic density and refined isotropically. Table I gives the pertinent crystallographic data. CCDC 277051 contains the supplementary crystallographic data for this paper. These data can be obtained free of charge via www.ccdc.cam.ac.uk/conts/retrieving.html (or from the Cambridge Crystallographic Data Centre, 12, Union Road, Cambridge, CB2 1EZ, UK; fax: +44 1223 336033; or deposit@ccdc.cam.ac.uk).

Chemicals and Stock Solutions for Potentiometric Titrations

The stock solution of hydrochloric acid (~0.03 mol l^{-1}) was prepared from 35% aqueous solution (puriss, Fluka). Commercial NMe_4Cl (99%, Fluka) was recrystallized from boiling *i*-PrOH and the solid salt was dried over P_2O_5 in vacuum to constant weight (this dried form of the salt is extremely hygroscopic). Carbonate-free NMe_4OH solution (~0.2 mol l^{-1}) was

prepared from NMe_4Cl using ion exchanger Dowex 1 in the OH^--form (elution with carbonate-free water, under argon) The hydroxide solution was standardized against potassium hydrogen phthalate and the HCl solution against the ca. 0.2 M NMe_4OH solution. Stock solutions of the individual metal cations were prepared by dissolving hydrates of $LnCl_3$ (99.9%; Strem) or dried NaCl (Fluka). The lanthanide(III) contents in the solutions were determined by titration with a standard Na_2H_2edta solution. Analytical concentration of a stock solution of the ligand was determined together with refinement of protonation constants using OPIUM software package (see below).

TABLE I
Experimental data for determination of the crystal structure of H_5do3ap·$4H_2O$

Formula	$C_{15}H_{37}N_4O_{13}P$
M	512.46
T, K	150(1)
Crystal dimension, mm	0.35 × 0.30 × 0.23
Colour and shape	colourless prism
Crystal system	monoclinic
Space group	$P2_1/c$ (No. 14)
a, Å	17.2904(4)
b, Å	7.9151(2)
c, Å	18.2587(4)
β, °	116.5595(14)
U, Å^3	2235.05(9)
Z	4
D_c, g cm^{-3}	1.523
λ, Å	0.71073
μ, mm^{-1}	0.198
F(000)	1096
θ range of data collection, °	2.91–27.49
Index ranges	$0 < h < 22$; $0 < k < 10$; $-23 < l < 21$
Data, restraints, parameters	5132; 0; 449
GOF on F^2	1.058
wR (all data), *wR*′ ([$I > 2\sigma(I)$])[a]	0.1188; 0.1106
R (all data), *R*′ ([$I > 2\sigma(I)$])[b]	0.0531; 0.0419
Largest difference peak and hole, e Å^{-3}	0.362; –0.522

[a] $wR = [\Sigma w(F_o^2 - F_c^2)^2/\Sigma w(F_o^2)^2]^{1/2}$, $w = 1/[\sigma^2(F_o^2) + (AP)^2 + BP]$; where $P = (F_o^2 + 2F_c^2)/3$ (SHELXL97, ref.[27]). [b] $R = \Sigma|F_o - F_c|/\Sigma|F_c|$ (SHELXL97, ref.[27]).

Potentiometric Titrations

Titrations were carried out in a vessel thermostatted at 25.0 ± 0.1 °C, at ionic strength I = 0.1 mol l^{-1} (NMe_4Cl) and in the presence of extra HCl in the pH range 1.7–11.9 (protonation constants and complex with Na^+) using a PHM 240 pH-meter, a 2-ml ABU 900 automatic piston burette and a GK 2401B combined electrode (all Radiometer, Denmark). The initial volume was 5 ml and the concentration of the ligand was ~0.004 mol l^{-1}. For Na^+-ligand system, the M:L = 10:1 molar ratio was used. Five parallel titrations were carried out; each titration consisted of about 40 points. An inert atmosphere was ensured by constant passage of argon saturated with the solvent vapour.

Titrations with lanthanide(III) ions were performed at metal-to-ligand molar ratios 1:1 and 2:1. As the complexation was too slow for conventional titration, the "out-of-cell" method was used. Each titration consisted of 23–25 points in the pH range 1.8–6.0 (at least two titrations for each 1:1 and 2:1 metal-to-ligand ratio). Equilibrium was reached after 30 days. The constants determined by this technique showed higher standard deviations due to less precise measurements and a smaller number of experimental points.

To find value of the third protonation constants of the lanthanide(III) complexes, useful for interpretation of NMR [20a] and kinetic data (below), we employed their high kinetic inertness in acid-assisted decomplexation. Stock solutions of $[Ln(do3ap)]^{2-}$ complexes were prepared (in ampoules) from $LnCl_3$ and the ligand stock solutions (with 5–10% ligand excess) by gradual neutralization with the stock NMe_4OH solution to pH ~ 7 (necessary amounts of the hydroxide and delays between its additions were estimated from a blank titration). The ampoules were sealed, heated at 50 °C for 5 h and left at room temperature for 24 h to ensure complete complexation. A known amount of the solutions was diluted, acidified and immediately titrated in the pH range 1.8–11.9 under the conditions mentioned above (0.1 M NMe_4Cl, 25 °C). The titrations performed in this way were well reproducible. However, the values of the constants determined by this technique are less correct, as concentrations of all components are known with smaller precision due to dilution errors.

The constants (with standard deviations) were calculated with program OPIUM [28]. The program minimizes the criterion of the generalized least-squares method using the calibration function (*1*)

$$E = E_0 + S\log[H^+] + j_1[H^+] + j_2K_w/[H^+] \quad (1)$$

where the additive term E_0 contains the standard potentials of the electrodes used and contributions of inert ions to the liquid-junction potential, S corresponds to the Nernstian slope, the value of which should be close to the theoretical value and the $j_1[H^+]$ and $j_2[OH^-]$ terms are the contributions of the H^+ and OH^- ions to the liquid-junction potential. It is clear that j_1 and j_2 cause deviation from a linear dependence of E on pH only in strongly acidic and strongly alkaline solutions. The calibration parameters were determined from titration of standard HCl with standard NMe_4OH before each ligand or ligand–metal titration to give a pair of calibration/titration, which was used for calculations of the constants. The protonation constants β_n are concentration constants, defined by $\beta_n = [H_nL]/([H]^n[L])$ (they were transformed to dissociation constants as $pK_1 = \log \beta_1$ and $pK_n = \log \beta_n - \log \beta_{n-1}$). The (concentration) stability constant are defined by $\beta_{hlm} = [H_hL_lM_m]/([H]^h[L]^l[M]^m)$. The water ion product pK_w (13.81) and stability constants of Ln^{3+}–OH^- systems included into the calculations were taken from refs[29,30].

NMR Titrations

The $^{31}P\{^1H\}$ NMR titration experiment for determination of the highest protonation constant (pH range 12.5–13.6, about 30 points) was carried out under the conditions close to the potentiometric titrations (0.1 M $NMe_4(Cl,OH)$; no control of ionic strength at points over pH > 13, 25.0 °C, ligand concentration ~0.004 mol l^{-1}). A coaxial capillary tube with D_2O was used for the lock. Protonation contants were calculated with OPIUM [28] from δ_P of the phosphonate group. NMR titrations over the whole pH region were performed at 25.0 °C in H_2O at ligand concentration 0.05 mol l^{-1} and with presaturation of water signal using a coaxial capillary with D_2O for the lock. Solution pH (0–14) was adjusted with aqueous NaOH or HCl solutions and measured with a pH-meter calibrated with standard buffers[31].

Kinetic Measurements

All measurements were carried out on a HP 8453A diode-array spectrophotometer at 25.0 ± 0.1 °C. Kinetics of formation of the $[Ce(do3ap)]^{2-}$ complex was followed under pseudo-first order conditions employing $c(Ce^{3+}) = (0.8–4.0) \times 10^{-3}$ and $c(H_5do3ap) = 8.0 \times 10^{-5}$ mol l^{-1}, $I = 0.1$ mol l^{-1} (KCl) in the pH range 4.0–5.5 (0.01 mol l^{-1} acetate buffer). Electronic spectra were collected in the UV region 290–340 nm. To visualize formation of $[Gd(do3ap)]^{2-}$ and to eliminate possible hydrolysis of Gd^{3+} ion, the chromogenic reagent Arsenazo III (2,7-bis-(2-arsonophenylazo)-1,8-dihydroxynaphthalene-3,6-disulfonic acid, H_8AZ; Fluka) was used[32]. Arsenazo III was used for determination of concentration of free gadolinium(III) in the course of formation of Gd^{3+} complex of H_3do3a (ref.[32]). The kinetics of formation of the $[Gd(do3ap)]^{2-}$ complex was followed under pseudo-first order conditions at $c(Gd^{3+}) = 1.7 \times 10^{-6}$ mol l^{-1}, $c(H_5do3ap) = 1.7 \times 10^{-5}$ mol l^{-1}, $c(H_8AZ) = (1.7–6.0) \times 10^{-6}$ mol l^{-1} and $I = 0.1$ mol l^{-1} (KCl) in the pH range 5.3–7.0 (0.01 M 2-morpholineethane-1-sulfonic acid, MES). Spectral changes were followed in the wavelength region 450–700 nm. The effect of the Gd^{3+}–Arsenazo III complex on the reactivity of the whole system was eliminated by extrapolation of the dependence of the observed pseudo-first order constants ${}^{Gd}k'_{f,obs}$ on the Arsenazo III concentration to the $c(H_8AZ) = 0$ (the explanation is given in Results and Discussion). Comparison of this procedure with a standard method (i.e., measurement of absorbance of the evolved coloured complex as in the case of Eu^{3+}) gave results with a satisfactory precision[33]. Recently, we observed also a good agreement between both methods for yttrium(III) complexation with H_3do3a (refs[32,34]).

Dissociation kinetics of the $[Ln(do3ap)]^{2-}$ complexes (Ln = Ce and Gd) were measured in the range of proton concentration 0.011–3.00 mol l^{-1} and at ionic strength $I = 3.0$ mol l^{-1} ($(Na,H)ClO_4$) with $c([Ce(L)]) = 1.0 \times 10^{-3}$ mol l^{-1} and $c([Gd(L)]) = 8.3 \times 10^{-5}$ mol l^{-1}. The decomplexation was followed by a decrease in the charge-transfer (CT) band of $[Ce(do3ap)]^{2-}$ at 315 nm or an increase in absorbance (665 nm) of the Gd^{3+}–H_8AZ complex formed as was proposed in the literature[32a]. The method was verified for the coloured europium(III) complex of H_5do3ap and the agreement between the results obtained by both methods was satisfactory[33]. The data from the kinetic experiments were processed by non-linear regression using Excel and Hewlett–Packard software with identical results. The measured values of absorbance were corrected for the background signal.

RESULTS AND DISCUSSION

Crystal Structure of $H_5do3ap·4H_2O$

The ligand H_5do3ap is highly soluble in water; originally, it was prepared in the solid state only by precipitation with anhydrous EtOH [20a]. It forms very easily oversaturated aqueous solutions. A long standing of such oversaturated solution led to a slow crystallization of $H_5do3ap·4H_2O$. A single crystal of the hydrate was used for determination of the solid-state structure. Conditions of the measurement and structural and fitting parameters are given in Table I. Important atom distances and angles are presented in Table II and the molecular structure of the ligand with the atom numbering scheme is shown in Fig. 1.

TABLE II
Geometry of the phosphonate group in the structure of $H_5do3ap·4H_2O$

	Distance, Å		Angles, °
P1–O1	1.5752(15)	O1–P1–O2	109.02(9)
P1–O2	1.5000(14)	O1–P1–O3	110.68(11)
P1–O3	1.4785(16)	O2–P1–O3	118.42(9)
P1–C13	1.8152(17)	C13–P1–O1	102.84(9)
		C13–P1–O2	104.52(8)
		C13–P1–O3	110.08(10)

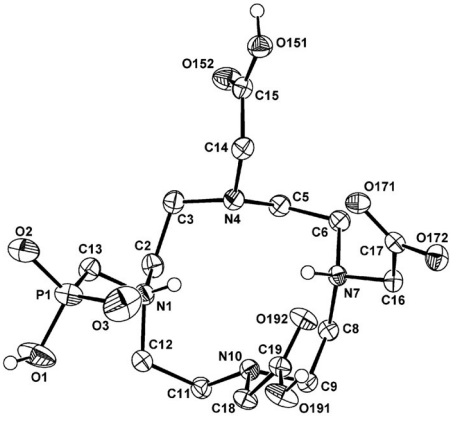

FIG. 1
A molecule in the crystal structure of the ligand $H_5do3ap·4H_2O$ with atom numbering scheme

The ligand crystallized as a free acid. The zwitterion structure with diprotonated cyclen ring is the most common feature of tetraazacycles with acid pendant arms crystallized from solutions of intermediate pH. Protonation of the nitrogen atom nearest to the phosphonate group is expected as partly or fully deprotonated phosphonic acid group spread electron density to the nearest amine group. The second proton is bound to the opposite nitrogen atom across the ring to minimize electrostatic repulsion. The remaining three protons are bound to phosphonate oxygen O1 and two carboxylic functions attached to non-protonated nitrogen atom of the cycle. This mode of protonation is preserved in aqueous solution for the H_5do3ap species (see below). The cyclen ring is in a common square conformation (3,3,3,3)-B with carbon atoms in the corners[6]. All four pendant substituents are facing the same side of the ring. The conformation of the ring is stabilized by intermediate (donor–acceptor contacts about 3 Å) hydrogen bonds between nitrogen atoms N1···N4 and N7···N10 (Table III). A rather long intramolecular hydrogen contact was found between N7 and oxygen atom O192 of the neighbouring acetate group. Intermolecular hydrogen bonds are also present in the structure of H_5do3ap·4H_2O, creating a network between the ligand and the water molecules of hydration.

Contrary to protonation of amino group bearing the phosphonate moiety, another mode of the protonation was found for an analogous phosphinate in the solid state[35]. In this case, two protons attached to amino groups were localized on two mutually trans nitrogen atoms each bearing acetate pendants. This confirms the higher basicity of nitrogen atoms in aminophosphonic acids compared with aminophosphinates[7]. Structural parameters of the phosphonate group in H_5do3ap are almost the same as those of the deprotonated phosphonate groups in solid state structure of H_8dotp (ref.[36]).

TABLE III
Intramolecular hydrogen bonds in the structure of H_5do3ap·4H_2O

D–H	*d*(D–H), Å	*d*(H···A), Å	< DHA, °	*d*(D···A), Å	A
N1–H11	0.86(2)	2.61(2)	111(2)	3.021(2)	N4
N7–H71	0.87(2)	2.56(2)	110(1)	2.978(2)	N10
N7–H71	0.87(2)	2.51(2)	125(1)	3.090(2)	O192

Protonation of H_5do3ap

Protonation (dissociation) constants (Table IV) of the title ligand were determined at 25 °C with NMe_4Cl as background salt due to possible formation of stable alkali metal ion complexes[37] (see also below). The last dissociation constant (pK_A 13.83) could not be found by means of potentiometry, instead, it was determined by ^{31}P NMR spectrometry. The high basicity was also observed for other acyclic[38] and macrocyclic[11,12,14,39,40] polyaminopolyphosphonic acids (see Table IV). This was ascribed to the effect of spreading the high electron density of the fully deprotonated phosphonate group to the nearest nitrogen atom(s)[7,41] or to the formation of the strong hydrogen bonds over ethylene chain[39]. Similar effects, though much less pronounced, lead also to a slight increase in pK_A corresponding to the sec-

TABLE IV
Dissociation and corresponding protonation constants of H_5do3ap and similar ligands

Ligand	pK_1	pK_2	pK_3	pK_4	pK_5	pK_6	pK_7	ΣpK_a[a]	Ref.
H_5do3ap[b]	13.83(4)[c]	10.35	6.54	4.34	3.09	1.63	1.07	35.06	this work
		10.35(1)	*16.89(2)*	*21.23(2)*	*24.32(2)*	*25.95(3)*	*27.02(8)*		
H_4dota	12.09	9.76	4.56	4.09	–	–	–	30.50	42
	12.6	9.70	4.50	4.14	2.32	–	–	30.9	43
	11.74	9.76	4.68	4.11	2.37	–	–	30.29	37
	11.45	9.64	4.60	4.11	2.29	–	–	29.80	44
H_8dotp[d]	13.7	12.2	9.28	8.09	6.12	5.22	–	43.3	11b
	–	12.5	9.25	8.01	6.17	5.17	1.77	–	11a
	12.8	12.3	8.90	7.75	5.95	5.14	1.77	41.75	14
H_4dotp^H[e]	10.41	6.83	1.97	–	–	–	–	–	15b
H_4dotp^{Ph}[f]	11.44	7.27	2.75	1.45	–	–	–	22.91	15c
H_4do2p[g]	12.80	10.92	8.47	6.39	–	–	–	38.58	45
H_4te2p[h]	26.41[i]		6.78	5.36	1.15	–	–	38.55	39

[a] ΣpK_A = pK_1 + pK_2 + pK_3 + pK_4. [b] Protonation constants (log β_n) determined by potentiometry are in italics (25 °C, 0.1 M NMe_4Cl). [c] Determined by ^{31}P NMR spectroscopy (25 °C, NMe_4(Cl,OH), no control of ionic strength). [d] H_8dotp = 1,4,7,10-tetraazacyclododecane-1,4,7,10-tetrakis(methylphosphonic acid); Chart 1. [e] H_4dotp^H = 1,4,7,10-tetraazacyclododecane-1,4,7,10-tetrakis(methylphosphinic acid); Chart 1. [f] H_4dotp^{Ph} = 1,4,7,10-tetraazacyclododecane-1,4,7,10-tetrakis[methyl(phenyl)phosphinic acid]; Chart 1. [g] H_4do2p = 1,4,7,10-tetraazacyclododecane-1,7-bis(methylphosphonic acid); Chart 1. [h] H_4te2p = 1,4,8,11-tetraazacyclotetradecane-1,8-bis(methylphosphonic acid); Chart 1. [i] Protonation over two steps.

ond protonation (10.35) in comparison with the value for H_4dota (~9.7; refs[37,42–44]). The next proton should be localized on the phosphonate moiety and the corresponding pK_A value (6.54) is similar to those for the other macrocyclic aminophosphonic acid ligands[39]. The other pK_A values are similar to those for H_4dota and should be assigned to protonations of acetate groups. The overall basicity of the ligands (as the sum of the first four pK_A values; Table IV) changes in the expected order[7,41]: phosphonates > acetates > phosphinates. Abundance of the differently protonated forms of the title ligand in an aqueous solution is shown in Fig. 2.

To determine sites of protonation of different ligand species in solution, we investigated the dependence of δ_H and δ_P on solution pH. Unfortunately, ^{1}H NMR spectra at almost all pH values were too broad and complicated to assign resonances to a particular proton, except the doublet of the N–CH_2–P group. The dependences of NMR parameters on pH are shown in Fig. 3. Even this limited set of data can be used for determination of the protonation sequence. It could be estimated on the basis of a number of such data published for aminoalkylphosphonic acids[38,46] and azamacrocycles with phosphonic acid pendant arm(s)[39,45,47,48]. The first protonation takes place at a very high pH (>13) and the proton should be attached to nitrogen atom of the ring. As δ_P is almost not changed at pH > 12, the proton

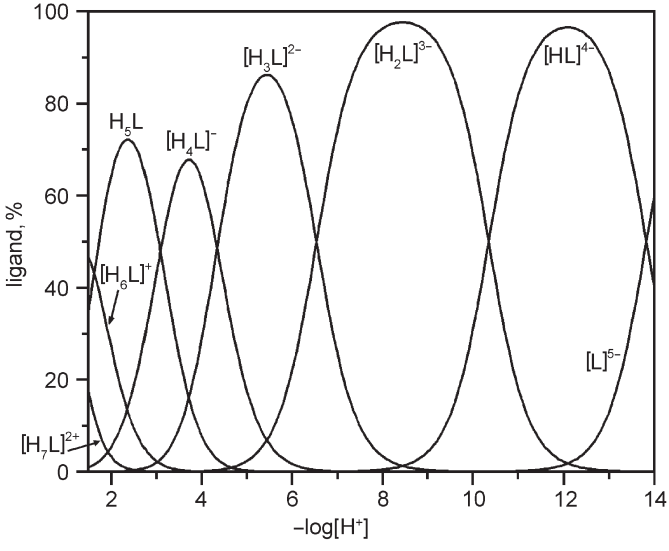

FIG. 2
Distribution diagram of H_5do3ap (Chart 1)

may reside on the nitrogen atom with acetate pendant adjacent to the N–CH_2–P group (Scheme 1). Such mode of protonation has been well documented for highly basic phosphonic acid derivatives of cyclam[39]. Attachment of the second proton leads to protonation of the nitrogen atom bearing the pendant phosphonate, as δ_P steeply falls down and δ_H rises. Because of electrostatic repulsion, the other proton must be bound to the opposite nitrogen atom. The characteristic steep change of δ_P with protonation of nitrogen atom of the N–CH_2–PO_3^{2-} moiety has been known for a long time[38,39,45–48]. The next protonation takes place at the phosphonate group. It leads to a redistribution of both protons already bound to ring to the opposite nitrogen atoms bearing acetate pendants (Scheme 1). This is supported by a large change in δ_P that is much higher than expected for pure

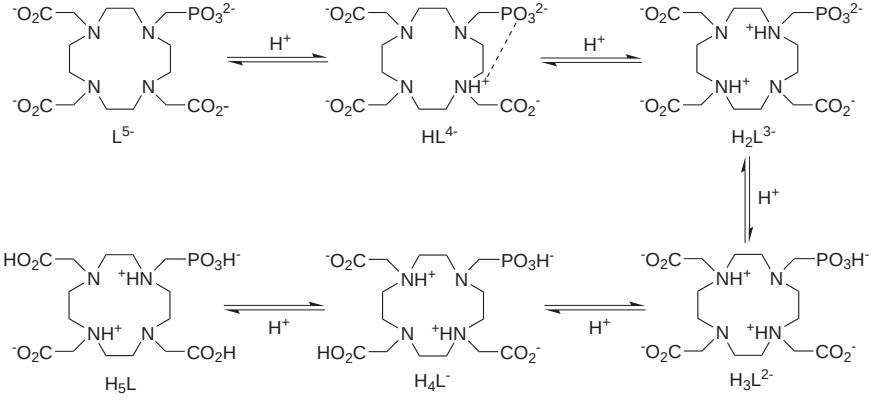

SCHEME 1
Protonation of H_5do3ap

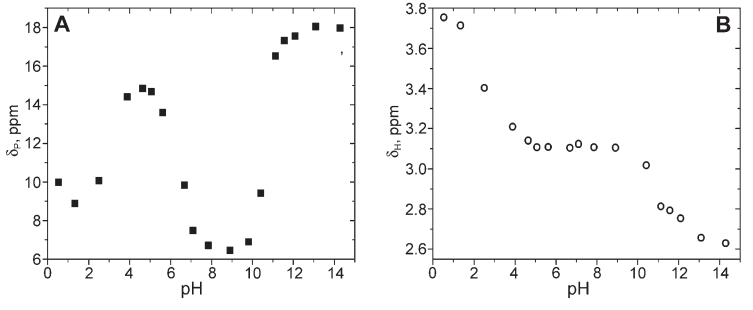

FIG. 3
pH dependence of δ_P (A) and δ_H (NC**H**$_2$P protons; B)

protonation of a phosphorus acid group. Such increase in δ_P is better explained by a concomitant deprotonation of the α-nitrogen atom. The δ_H is not changed in this region, as the effects of deprotonation of the close nitrogen atom and protonation of the phosphonate group cancel each other. Comparing pK_A values with those for similar ligands, the next two protonations should take place on the pendant acetate groups. As there is almost no change in δ_P and δ_H at pH 4–5, the fourth proton should be associated with the acetate group opposite to the $N–CH_2–PO_3H^-$ moiety. Addition of the fifth proton leads to another redistribution of protons as δ_P as well as δ_H change. A decrease in δ_P indicates a repeated protonation of the $N–CH_2PO_3H^-$ nitrogen atom and, therefore, the opposite nitrogen atom must be also protonated again. Then, the most stable arrangement should be that with protonated acetate groups attached to N4 and N10 (Scheme 1). Exactly the same protonation of the species H_5do3ap was observed in the solid state (see above). Sites of the next protonations cannot be assigned with the available data; however, ring nitrogen atoms should be fully protonated only in a highly concentrated acid.

Thermodynamic Stability of Metal Complexes of H_5do3ap

Stability constants were determined by potentiometric titrations and the experimental values (log β_{hlm}) are given in Table V. The selected derived stability constants and their comparison with those for H_4dota and H_8dotp are listed in Table VI. The use of NMe_4Cl as background electrolyte was justified by a measurable formation of the $[Na(do3ap)]^{4-}$ complex that is slightly more stable (log β_{NaL} = 4.77) than the corresponding complex of H_4dota (log $\beta_{Na(dota)}$ = 4.38 (ref.[42]); 4.03 (ref.[37])).

Complexes of lanthanide(III) ions with H_5do3ap exhibit the same solution and the solid state structures as these of H_4dota[20]. Therefore, the fully deprotonated complexes should be correctly formulated as $[Ln(H_2O)(do3ap)]^{2-}$ (ref.[23]). The ligand wraps the ions in an octadentate square-antiprismatic fashion by four nitrogen atoms below and four oxygen atoms of the pendant arms above the central ion. From the Table VI, it is clear that lanthanide(III) complexes of H_5do3ap are more stable than those of H_4dota but less stable than those of H_8dotp. This corresponds with the previous assumption[7] that values of stability constants of such ligands depend principally on the basicity of the ring nitrogen atoms.

The first proton (Table VI) is attached to the phosphonate group without changed coordination mode of the ligand[20], forming $[Ln(Hdo3ap)]^-$; the

TABLE V
Stability constants (log β_{hlm}) of complexes of H_5do3ap with Na^+, Ln^{3+} and Y^{3+} [a]

Metal ion	*h l m*					
	4 1 1	3 1 1	1 1 1	0 1 1	1 1 2	0 1 2
Na^+	–	–	–	4.77(3)	–	–
La^{3+}	38.3(1)	36.46(2)	30.84(3)	25.5(1)	–	28.3(2)
Ce^{3+}	–	36.67(3)	31.96(2)	26.5(1)	–	29.5(5)
Eu^{3+}	–	37.26(5)	33.33(2)	27.8(1)	35.64(9)	32.0(1)
Gd^{3+}	–	36.91(5)	33.06(2)	27.50(9)	35.1(1)	31.6(1)
Lu^{3+}	–	37.35(7)	33.79(3)	28.6(1)	–	32.9(1)
Y^{3+}	–	36.78(2)	31.70(2)	26.0(2)	–	30.0(2)

[a] Determined by the "out-of-cell" method, except for Na^+ (see Experimental).

TABLE VI
Selected equilibrium constants derived for complexes of H_5do3ap and related ligands with Ln^{3+} and Y^{3+} ions

Equilibrium	log (corresponding equilibrium constant) or pK_a					
	ligand	La^{3+}	Ce^{3+}	Eu^{3+}	Gd^{3+}	Lu^{3+}	Y^{3+}
$M + L \rightleftharpoons [M(L)]$	H_5do3ap	25.5	26.5	27.8	27.5	28.6	26.0
	H_4dota	22.9[b]	24.6[c]	24.7[b]	24.7[b]	25.4[b]	–
				26.48[d]	24.67[e]		
					25.58[d]		
	H_8dotp[f]	27.6	27.7	28.1	28.8	29.6	–
$[M(HL)] \rightleftharpoons [M(L)] + H$	H_5do3ap	5.3	5.5	5.5	5.6	5.2	5.7
	H_4dota	–	1.9[c]	–	–	–	–
	H_8dotp[f]	–	7.7	–	7.6	8.7	–
$[M(H_3L)] \rightleftharpoons [M(HL)] + 2H$	H_5do3ap	5.62	4.71	3.93	3.85	3.56	5.08
		"2×2.81"	"2×2.36"	"2×1.97"	"2×1.93"	"2×1.78"	"2×2.54"
	H_4dota[g]	–	–	2.62	2.68	–	–
$H_3L + M \rightleftharpoons [M(H_3L)]$	H_5do3ap	5.74	5.95	6.54	6.19	6.63	6.06
	H_4dota[h]	–	–	8.26	9.32	–	–
$[M(L)] + M \rightleftharpoons [M_2(L)]$	H_5do3ap	2.8	3.0	4.2	4.1	4.3	4.0

[a] Charges are omitted for clarity; [b] Ref.[49]; [c] ref.[43]; [d] ref.[44]; [e] ref.[37]; [f] ref.[11a]; [g] pK_A for the first dissociation of the transient equilibrium complex [Ln(H_2dota)]* (ref.[44]); [h] Corresponding equilibrium constant for formation of the transient equilibrium complex (H_2dota + Ln $\rightleftharpoons$ [Ln(H_2dota)]*) (ref.[44]).

values of the corresponding pK_1 are in the range 5.2–5.7. The values are in the similar range as those of $[Ln(dotp)]^{5-}$ where four pK_A's (corresponding to protonation of four phosphonate groups) spanning from 4 to 9 were determined[11b]. Surprisingly, $[Ln(H_2do3ap)]$ species could not be included into any chemical model but triprotonated species $[Ln(H_3do3ap)]^+$ had to be involved. Considering the commonly accepted mechanism of formation of H_4dota lanthanide(III) complexes[44,50–52] (see also below), these species may be expected. In the mechanism, lanthanide(III) ions are rapidly bound to the oxygen atoms of the pendant arms while two protons are still bound to two ring nitrogen atoms. The following slow base-catalyzed isomerization leads to the final complex with an octadentate ligand mode. Complex species with a doubly protonated ligand (e.g. H_4dota) have not been included in any final equilibrium model but, they were proved as intermediates under non-equilibrium conditions[44]. Furthermore, because of the ability of the (protonated) phosphonate moiety to coordinate lanthanide(III) ions in acidic solutions[53] and very high basicity of nitrogen atom(s) of H_5do3ap, the $[Ln(H_3do3ap)]^+$ species could be detected in our equilibrium mixture (protonated probably on two nitrogen atoms and on the phosphonate group). The presence of the species in acidic solutions (Fig. 4, A–C) indirectly confirms the mechanism of complexation given below. However, exact sites of protonation and their fractions need not be necessarilly the same in the thermodynamic species and in the kinetic intermediate species (see below). The species could be compared with the protonated transient complexes involved in the mechanism of formation of $[Ln(dota)]^-$ (marked commonly with asterisk, $[Ln(H_2dota)]^{*+}$)[44]. The formation constants of $[Ln(H_3do3ap)]^+$ species are lower than those of $[Ln(H_2dota)]^{*+}$ species, but we have to take into account that our complexes contain three protons. The "pK_A" values (1.8–2.8) of $[Ln(H_3do3ap)]^+$ species are lower than those of $[Ln(H_2dota)]^{*+}$ but, again, they have been determined over two steps and should involve a contribution of deprotonation of the amines/carboxylates together with possible proton transfer to already coordinated phosphonate group of a lower acidity (see also the kinetic part below).

In solutions with an excess of metal ion, complexes with the $[Ln_2L]^+$ stoichiometry were detected. Stabilities of the dinuclear complexes are comparable with those of commonly used lanthanide(III) metal indicators such as Xylenol Orange[29]. The indicators are used for testing the presence of any small excess of lanthanide(III) ions in solutions for NMR measurements used to determine parameters relevant to investigations of new contrast agents for MRI (presence of uncomplexed metal ions is highly undesirable). However, if the metal ion is present in solution only in a small excess and

such dinuclear complexes with H_4dota-like ligands are formed, the small excess of the lanthanide(III) ion then may not be detected with these indicators. The finding should be considered while preparing samples for such NMR measurements[20a].

It was observed that some solution properties (e.g., abundance of different diastereoisomers) of $[Ln(do3ap)]^{2-}$ complexes with heavier lanthanides (Eu–Tm) highly depend on pH of solution (i.e., on the protonation state of the complexes)[20a]. Therefore, it was interesting to determine protonation constants of the complexes. The knowledge of these constants is also useful for the interpretation of data from acid-assisted dissociation of the complexes (therefore, the light lanthanide ion Ce^{3+} was also included in the study). As the complexes are only slowly decomposed in acidic solutions (see below), preformed complexes may be titrated starting from acidic solutions. The protonation (dissociation) constants of the complexes studied

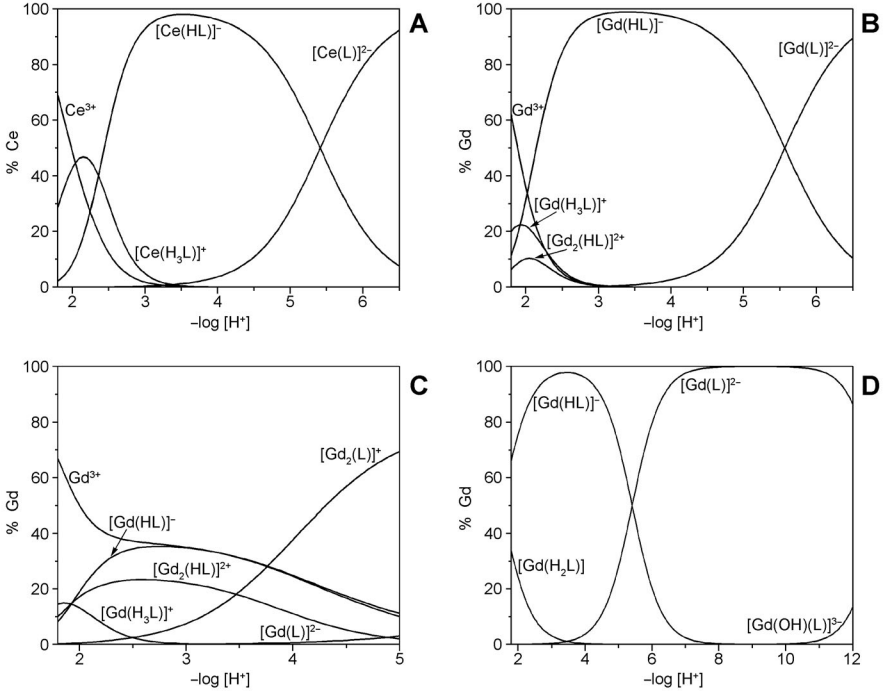

FIG. 4

Distribution diagrams for Ln^{3+}–H_5do3ap systems: $c(Ce^{3+}) = c(H_5L) = 0.004$ mol l^{-1} (A); $c(Gd^{3+}) = c(H_5L) = 0.004$ mol l^{-1} (B); $c(Gd^{3+}) = 0.008$ mol l^{-1}, $c(H_5L) = 0.004$ mol l^{-1} (C); speciation obtained after titration of preformed $[Gd(do3ap)]^{2-}$ (D)

are given in Table VII. The first protonation (pK_1) takes place on non-coordinated phosphonate oxygen atom and, therefore, the pK_1 values should be the same as under equilibrium conditions. Indeed, reasonable agreement between the values (5.2–5.7 (Table VI) and 5.2–5.4 (Table VII), respectively) was found. The second proton should be attached to an oxygen atom of any group still coordinated to the central ion in the complex that does not decompose during the titration. This is a difference from equilibrium conditions (above) where no diprotonated species could be involved in chemical model. Under equilibrium conditions, the found triprotonated species bind lanthanide(III) ions mainly through the pendant arms and two nitrogen atoms should be protonated (see above). Protonation of coordinated carboxylate groups was proved for $[Ln(dota)]^-$ (Ln = La, Y), although, under different conditions (2.0 M (H,Na)Cl, 5 °C)[54]. Thus, the found values of pK_A (0.96 and 0.95 for La^{3+} and Y^{3+}, respectively) are slightly lower than those determined for complexes of H_5do3ap. The pK_A values very similar to those for $[Ln(do3ap)]^{2-}$ complexes were found for protonation of the second phosphonate oxygen atom in the preformed complexes of H_4te2p with cobalt(III)[55], nickel(II)[56] and copper(II)[57] (pK_A =

TABLE VII
Protonation and *dissociation* constants of several $[Ln(H_2O)(do3ap)]^{2-}$ complexes[a]

Metal ion	$\log \beta_{2Ln}$	$\log \beta_{1Ln}$	$\log \beta_{-1Ln}$[b]
Ce^{3+}	6.75(3)	5.22(2)	–12.30(3)
	1.53	*5.22*	
Eu^{3+}	6.91(2)	5.41(1)	–12.79(3)
	1.50	*5.41*	
Gd^{3+}	6.81(4)	5.42(2)	–12.72(4)
	1.39	*5.42*	
Tb^{3+}	6.92(4)	5.42(2)	–12.66(6)
	1.50	*5.42*	
Ho^{3+}	7.04(3)	5.40(2)	–12.73(5)
	1.64	*5.40*	
Er^{3+}	6.93(2)	5.26(2)	–12.61(3)
	1.67	*5.26*	

[a] Determined by direct titration of the preformed complexes; see Experimental. [b] Values of the constants correspond to deprotonation of the coordinated water molecule.

1.15–1.87) under similar conditions (0.1 M KNO_3, 25 °C). Deprotonation of the coordinated water molecule takes place only in highly alkaline solution. A representative distribution diagram is shown in Fig. 4D.

Formation Kinetics

To investigate kinetic properties of lanthanide(III) complexes of H_5do3ap, Ce^{3+} and Gd^{3+} ions were chosen, as there is enough experimental data in the literature for analogous complexes with other ligands. The kinetics of formation of the Ce^{3+} complex was followed by UV-VIS spectroscopy. Typical absorption spectra of solution after mixing the reactants ($CeCl_3$ and H_5do3ap) as a function of time, are shown in Fig. 5A and kinetic traces at two chosen wavelengths are presented in Fig. 5B. The appearance of a characteristic absorption band of the final complex with maximum at about 313 nm could be noticed at the end of the reaction and an isosbestic point at about 306 nm was observed. A similar pattern was also recorded in the case of H_4dota [50,58]; however, in the H_4dota case, also the maximum of absorption band of an intermediate at about 297 nm was observed. In our case, only a small shoulder was observed at a similar wavelength (Fig. 5A).

The pseudo-first order reaction conditions were employed: 10–50 times higher concentration of Ce^{3+} over the ligand concentration. The rate law of complex formation can be written as shown in Eq. (*2*) (charges of complexes are omitted).

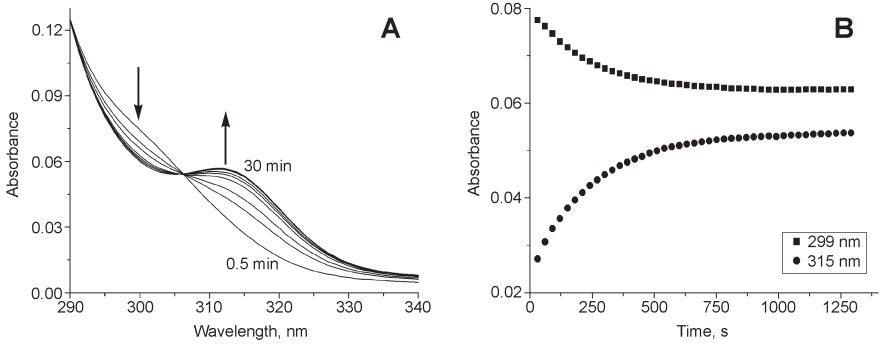

FIG. 5

An example of raw experimental data for the study of the kinetics of formation of the $[Ce(Hdo3ap)]^{-}/[Ce(do3ap)]^{2-}$ complexes. Conditions: $c(Ce^{3+}) = 1.6 \times 10^{-3}$ mol l^{-1}, $c(H_5do3ap) = 8 \times 10^{-5}$ mol l^{-1}, pH 5.3. Absorption spectra of the reaction mixture recorded at different times (A); time traces measured at chosen wavelengths (B)

$$\frac{d[Ce(L)]}{dt} = {}^{Ce}k_{f,obs}[ligand]_{tot} \quad (2)$$

The mostly used model of the complexation reaction assumes a fast formation of reaction intermediate which is in fast equilibrium with starting compounds and is characterized by conditional stability constant ${}^{Ce}K^{**}$.

$${}^{Ce}K^{**} = \frac{[Ce(H_3L)]}{[Ce^{3+}][ligand]_{tot}} \quad (3)$$

It is followed by the slow rate-determining step of the final product formation defined by rate constant ${}^{Ce}k_f$.

$${}^{Ce}k_{f,obs} = \frac{{}^{Ce}k_f\,{}^{Ce}K^{**}[Ce^{3+}]_{tot}}{1 + {}^{Ce}K^{**}[Ce^{3+}]_{tot}} \quad (4)$$

The conditional pseudo-first order rate constant ${}^{Ce}k_{f,obs}$ is dependent in this case on the analytical concentration of metal ion, i.e., $[Ce^{3+}]$.

The pseudo-first order rate constant ${}^{Ce}k_{f,obs}$ (for $c(Ce^{3+}) \geq 10c(H_5do3ap)$) was practically independent of the total Ce^{3+} concentration at pH 4.6 and 5.3, and the same effect was observed for a ligand excess (data not shown). This means that the formation of kinetic reaction intermediate is quantitative (${}^{Ce}K^{**}[Ce^{3+}]_{tot} >> 1$ in denominator, Eq. (*4*)), and the relationship can be simplified with the assumption as given in Eq. (*5*).

$${}^{Ce}k_{f,obs} = \frac{{}^{Ce}k_f\,{}^{Ce}K^{**}[Ce^{3+}]_{tot}}{1 + {}^{Ce}K^{**}[Ce^{3+}]_{tot}} \approx \frac{{}^{Ce}k_f\,{}^{Ce}K^{**}[Ce^{3+}]_{tot}}{{}^{Ce}K^{**}[Ce^{3+}]_{tot}} = {}^{Ce}k_f \quad (5)$$

Therefore, these experimental conditions were chosen for the measurements. The determined conditional equilibrium constant ${}^{Ce}K^{**}$ is dependent on the solution pH, while other protonated species of ligand are present in the solution[59,60] (Eq. (*6*), $K_{p,n}$ are consecutive ligand protonation constants) and, therefore, the equilibrium constant ${}^{Ce}K^{*}$ is defined by Eq. (*7*):

$${}^{Ce}K^{**} = \frac{[Ce(H_3L)]}{[Ce^{3+}][H_3L](1 + K_{p,4}[H^+] + K_{p,4}K_{p,5}[H^+]^2)} = \frac{{}^{Ce}K^{*}}{\alpha_{H_3L(H)}} \quad (6)$$

$$^{Ce}K^{*} = \frac{[Ce(H_3L)]}{[Ce^{3+}][H_3L]} \qquad (7)$$

The equilibrium constant $^{Ce}K^{**}$ (as a pH-dependent parameter) can be calculated from absorbance values extrapolated to zero time ($A_{t=0}$)[17,43,50]. The conditional equilibrium constant $^{Ce}K^{**}$ was corrected for ligand protonation according to Eq. (*6*) in order to calculate $^{Ce}K^{*}$, and the value of log ($^{Ce}K^{*}$) = 3.45 ± 0.04 was estimated. This value should be constant for the pH region employed in the study[50,59,60], corresponding to the stability constant for the intermediate species prevailing in solution under the given experimental conditions[50,59,60]. This requirement for the constant value of log ($^{Ce}K^{*}$) is not fulfilled for the [Ce(H_2L)]* species. Therefore, this species is probably only a minor one. The log ($^{Ce}K^{*}$) value for the [Ce(H_3L)]$^{*+}$ species lies between those reported for the corresponding Ce(H_2Lig)* species with H_4dota (4.5 ± 0.1)[50] and H_2do2a (1.98 ± 0.06)[60]. It is comparable to the constant found for corresponding Ce(HLig)* species with H_3nota (3.2 ± 0.1)[59]. Therefore, we can assume (on the basis of the previously published results for other macrocyclic ligands, mostly for H_2do2a and H_4dota)[50,60] that the composition of the kinetic reaction intermediate should be with [Ce(H_3do3ap)]$^{*+}$ as the major species and with [Ce(H_2do3ap)]* and/or [Ce(Hdo3ap)]$^{*-}$ as the minor ones. All intermediate species are in fast protonation equilibria (Scheme 2). This hypothesis is indirectly confirmed by the fact that the most abundant protonated species of ligand in the pH region 4–5.5 is H_3do3ap^{2-}.

The [Ce(H_3do3ap)]$^{+}$ species was found in equilibrium mixtures of Ln^{3+}–H_5do3ap systems (see above) and, at low pH, it is probably too stable (Table VI) to undergo further deprotonation reaction, as observed in the case of the Eu(III)–H_4dota system[44]. For the complexation, the double-protonated species [Ce(H_2L)] is therefore crucial. The presence of a similar intermediate species [Ce(H_2dota)]$^{*+}$ in an aqueous solution was also postulated (log K_2^{*} = 4.5 ± 0.1)[50]. The structure of the reaction intermediates is probably similar in both (H_5do3ap and H_4dota) cases, assuming a protonation of two nitrogen atoms of the cyclen ring. In the species [Ce(H_3do3ap)]$^{+}$, the third proton is probably attached to the phosphonate group coordinated to the lanthanide(III) ion. In addition, luminescent measurements on the Eu^{3+}–H_5do3ap system[33] proved that the Eu^{3+} ion in the intermediate species is coordinated by three water molecules and, thus, the coordination sphere of metal ion is completed with six donor atoms of the ligand (four oxygen atoms of all pendant arms and two non-protonated ni-

trogen atoms of the macrocycle). Recently, such double nitrogen protonation was observed in crystal structures of a series of $[Ln_2(H_2O)_2(H_2do3ap^{Ph})_2]^{2+}$ complexes crystallized from aqueous solutions at pH < 3 (for structure of H_4do3ap^{Ph}, see Chart 1)[61]. In contrast, a different structure (ligand protonated on one nitrogen atom) was predicted for complexation kinetics in yttrium(III)–H_4dota system by quantum mechanics[62]. The rate-limiting step of the whole formation reaction is the deprotonation of nitrogen atoms[43,44,51,60,62] catalyzed by hydroxide ions (Eq. (*8*), Fig. 6).

$$^{Ce}k_f = {}^{Ce}k_{f,obs} = {}^{Ce}k_{OH}[OH^-] \qquad (8)$$

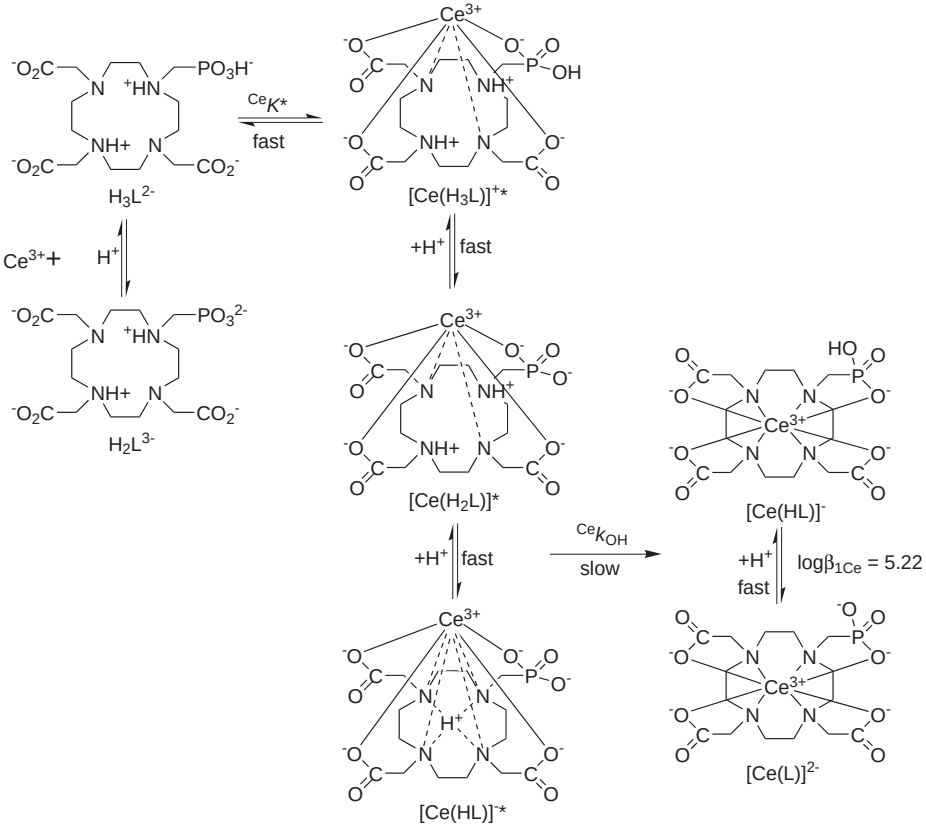

SCHEME 2

Proposed reaction mechanism for complexation of Ce^{3+} with H_5do3ap (sites of protonations are tentative)

The rate constant ${}^{Ce}k_{OH} = (9.56 \pm 0.28) \times 10^5$ l mol^{-1} s^{-1} is given by the slope of the linear dependence (Fig. 6). The following simplified reaction mechanism (Scheme 2) of the cerium(III) complex formation can be postulated analogously to the Ce^{3+}–H_4dota system[43]. The values of the rate constants k_{OH} for Ce^{3+}–H_4dota and Ce^{3+}–H_5do3ap systems are comparable (Table VIII). Therefore, the calculated values support the reaction mechanism discussed above.

As the Gd^{3+}–H_5do3ap system cannot be studied by the same method as the Ce^{3+}–H_5do3ap systems, it was necessary to employ an auxiliary chromogenic ligand Arsenazo III (H_8AZ). The exchange kinetics in the Eu^{3+}–Arsenazo III[65] and Gd^{3+}–Arsenazo III[66] systems with common polyaminocarboxylates were studied and reaction mechanisms were proposed. Gadolinium(III) forms with Arsenazo III complexes [M(AZ)] (ref.[67]) and some authors assume also [M(AZ)$_2$] (ref.[67a]) and [M$_2$(AZ)$_2$] (ref.[67a]) complexes, while formation of the dinuclear complex is favoured for higher overall concentrations of the metal ion and the dye (>5 ± 10^{-5} mol l^{-1})[67a].

Similarly to the Ce^{3+}–H_5do3ap system, the rate law for formation of the [Gd(do3ap)]$^{2-}$ complex under the pseudo-first order conditions ($c_L >> c_M$) can be postulated as Eqs (*9*) and (*10*), where ${}^{Gd}K^{**}$ is the conditional equilibrium constant for the formation of an intermediate complex defined analogously to the Ce^{3+}–H_5do3ap system (see Eqs (*6*) and (*7*)). However, the stoichiometry of the species is probably [Gd(H_2L)], as the consequence of a

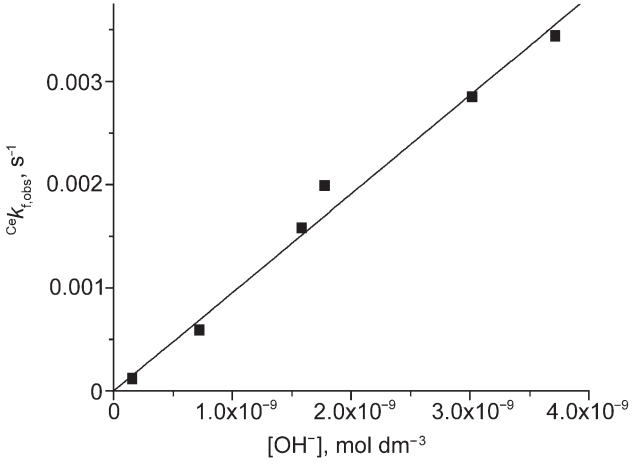

FIG. 6
The dependence of the observed pseudo-first order rate constant ${}^{Ce}k_{f,obs}$ on [OH$^-$] for the formation of [Ce(Hdo3ap)]$^-$/[Ce(do3ap)]$^{2-}$ complexes

TABLE VIII

The overview of rate constants of formation/dissociation reactions of lanthanide(III) complexes with cyclen derivatives (T = 25 °C; unless stated otherwise in text)

Ligand	Ce^{3+}		Gd^{3+}	
	formation[m]	dissociation[n,o]	formation[m]	dissociation[n,o]
H_2do2a[a]	k_{OH}=2.8×10^5 M^{-1}s^{-1} log K_2*=1.98 (ref.[60])[b]	–	–	–
H_3do3a[c]	–	k_{H1}=1.12×10^{-1} M^{-1}s^{-1} k_0=1.8×10^{-3} s^{-1} (ref.[32b])[d]	k_{OH}=2.1×10^7 M^{-1}s^{-1} (ref.[32c])[d]	k_{H1}=1.17×10^{-2} M^{-1}s^{-1} k_0=1.90×10^{-4} s^{-1} (ref.[32a])[e] k_1=7.4×10^{-3} M^{-1}s^{-1} k_0=4.4×10^{-4} s^{-1} K_2=3.6 M^{-1} (ref.[32b])[d]
H_4dota	k_{OH}=2.7×10^6 M^{-1}s^{-1} (ref.[43])[f]	k_{H1}=8×10^{-4} M^{-1}s^{-1} k_{H2}=2×10^{-3} M^{-2}s^{-1} (ref.[50])[g]	k_{OH}=5.9×10^6 M^{-1}s^{-1} (refs[32c,52])[d]	k_{H1}=2.0×10^{-5} M^{-1}s^{-1} k_0=5×10^{-10} s^{-1} (ref.[50])[g]
	k_{OH}=3.5×10^6 M^{-1}s^{-1} log K_2*=4.5 (ref.[50])[d]	k_{H1}=3.373×10^{-4} M^{-1}s^{-1} k_{H2}=1.605×10^{-3} M^{-2}s^{-1} (ref.[63])[h]		k_{H1}=8.4×10^{-6} M^{-1}s^{-1} k_0<5×10^{-8} s^{-1} (ref.[52])[d]
H_3do3a-hp[i]	–	k_{H1}=2.00×10^{-3} M^{-1}s^{-1} k_0=1.4×10^{-4} s^{-1} (ref.[32b])[d]	–	k_1=6.4×10^{-4} M^{-1}s^{-1} K_2=1.00 M^{-1} (ref.[32b])[d]
H_8dotp	–	k_{H1}=4.63×10^{-5} M^{-1}s^{-1} (ref.[64])[g]	k_{OH}=7.2×10^3 M^{-1}s^{-1} (refs[13])[f]	k_1=5.4×10^{-4} M^{-1}s^{-1} K_2=1.7 M^{-1} k_{H1}=9.18×10^{-4} M^{-1}s^{-1} (ref.[13])[i]
H_5do3ap[k]	k_{OH}=9.6×10^5 M^{-1}s^{-1} log K_3*=3.45	k_{H1}=1.22×10^{-3} M^{-1}s^{-1}	k_{OH}=9.0×10^4 M^{-1}s^{-1}	k_{H1}=2.78×10^{-3} M^{-1}s^{-1} $k_{d,2}$=5.8×10^{-2} M^{-1}s^{-1} $^H K_3$=0.048 M^{-1}

[a] H_2do2a = 1,4,7,10-tetraazacyclododecane-1,7-diacetic acid; Chart 1. [b] I: 1 M KCl. [c] H_3do3a = 1,4,7,10-tetraazacyclododecane-1,4,7-triacetic acid; Chart 1. [d] I: 1.0 M NaCl. [e] I: 0.5 M KNO_3. [f] I: 1 M Me_4NCl. [g] I: 3.0 M $NaClO_4$. [h] I: 1.0 M HCl/KCl. [i] H_3do3a-hp = 10-(2-hydroxypropyl)-1,4,7,10-tetraazacyclododecane-1,4,7-triacetic acid; Chart 1. [j] I: 1.0 M Me_4NCl. [k] This work: for formation, I: 0.1 M KCl; for dissociation, I: 3.0 M (H,Na)ClO_4. [l] T = 37 °C. [m] $k_{f,obs} = k_{OH}[OH^-]$; $K_n^* = \frac{[M(H_nL)]]}{[M^{3+}][H_nL]}$. [n] $k_{d,obs} = k_0 + k_{H1}[H^+] + k_{H2}[H^+]^2$. [o] $k_{d,obs} = k_0 + \frac{k_1[H^+]}{1 + K_2[H^+]}$.

higher pH range employed for the formation of the Gd^{3+} complexes (5.3–7.0) compared to that for the Ce^{3+} complexes (4.0–5.5).

$$\frac{d[Gd(L)]}{dt} = {}^{Gd}k_{f,obs}[Gd^{3+}]_{tot} \qquad (9)$$

$${}^{Gd}k_{f,obs} = \frac{{}^{Gd}k_f\,{}^{Gd}K^{**}[ligand]_{tot}}{1 + {}^{Gd}K^{**}[ligand]_{tot}} \qquad (10)$$

The presence of an additional ligand (Arsenazo III) inhibits the formation of the complex, as the concentration of the free metal ion decreases due to the formation of the Gd^{3+} complex with Arsenazo III (assuming that of Gd^{3+}–Arsenazo III complexes do not react with the macrocylic ligand, as transchelation is usually a relatively slow reaction)[66,67]. Thus, the conditional pseudo-first order rate constant ${}^{Gd}k'_{f,obs}$ is lower than ${}^{Gd}k_{f,obs}$ by a factor correcting the total concentration of Gd^{3+} to concentration of free Gd^{3+} ion (Eq. (*11*)).

$${}^{Gd}k'_{f,obs} = {}^{Gd}k_{f,obs}\delta_{Gd} = \frac{{}^{Gd}k_{f,obs}}{1 + {}^{A}K_1[AZ] + {}^{A}K_1\,{}^{A}K_2[AZ]^2} \qquad (11)$$

The constants ${}^{A}K_1$ and ${}^{A}K_2$ are equilibrium constants corresponding to the formation of Gd^{3+}–Arsenazo III complexes [M(AZ)] and [$M(AZ)_2$]. Equation (*12*) can easily be obtained by rearrangement of Eqs (*10*) and (*11*).

$${}^{Gd}k'_{f,obs} = \frac{{}^{Gd}k_f\,{}^{Gd}K^{**}[ligand]_{tot}}{1 + {}^{Gd}K^{**}[ligand]_{tot}} \cdot \frac{1}{1 + {}^{A}K_1[AZ] + {}^{A}K_1\,{}^{A}K_2[AZ]^2} \qquad (12)$$

A similar mathematical model was recently derived for the description of the inhibiting effect of zinc(II) complexes on phosphodiester cleavage[68]. If the measured pseudo-first order rate constant ${}^{Gd}k'_{f,obs}$ is extrapolated to zero concentration of the competing ligand (Arsenazo III), Eq. (*12*) is simplified to Eq. (*13*). In addition, if the stability constant of the intermediate ${}^{Gd}K^{**}$ is high (generally, it should be higher for $[Gd(H_2L)]^*$ species than for $[Gd(H_3L)]^{*+}$) and the employed experimental conditions are pseudo-first order (c(ligand) ≥ 10c(Gd^{3+})), one can suggest that ${}^{Gd}K^{**}([ligand]_{tot} >> 1$. Then, the formation rate can be given similarly as in the case of the Ce^{3+}–H_5do3ap system (Eq. (*13*)).

$$ {}^{Gd}k_{f,obs} = \frac{{}^{Gd}k_f\,{}^{Gd}K^{**}[\text{ligand}]_{tot}}{1+{}^{Gd}K^{**}[\text{ligand}]_{tot}} \approx \frac{{}^{Gd}k_f\,{}^{Gd}K^{**}[\text{ligand}]_{tot}}{{}^{Gd}K^{**}[\text{ligand}]_{tot}} = {}^{Gd}k_f \qquad (13) $$

The great benefit of the proposed experimental method is the fact that the rate of the formation reaction can be measured in the pH region where measurements by conventional spectroscopy are often impossible due to a very fast reaction. In addition, the sensitivity of the measurement are very high due to the strongly absorbing reagent that forms very stable complexes with lanthanide(III) ions, hence protecting them against hydrolysis at higher pH.

Application of Arsenazo III to measurement of kinetics of formation of the Gd^{3+}–H_5do3ap complex is demonstrated in Fig. 7. The dependence of the observed pseudo-first order rate constant ${}^{Gd}k'_{f,obs}$ on the concentration of Arsenazo III is strictly linear. It proves that only one relatively stable Gd^{3+}– Arsenazo III complex, probably of the Gd:AZ = 1:1 stoichiometry, is formed. The measured values of ${}^{Gd}k'_{f,obs}$ were extrapolated to zero concentration of Arsenazo III and these values were used for the calculation of the rate constant ${}^{Gd}k_{OH}$. As can be seen from Fig. 8, the dependence ${}^{Gd}k_{f,obs}$ on $[OH^-]$ is strictly linear (r^2 = 0.9897); it was fitted by a straight line using Eq. (*14*).

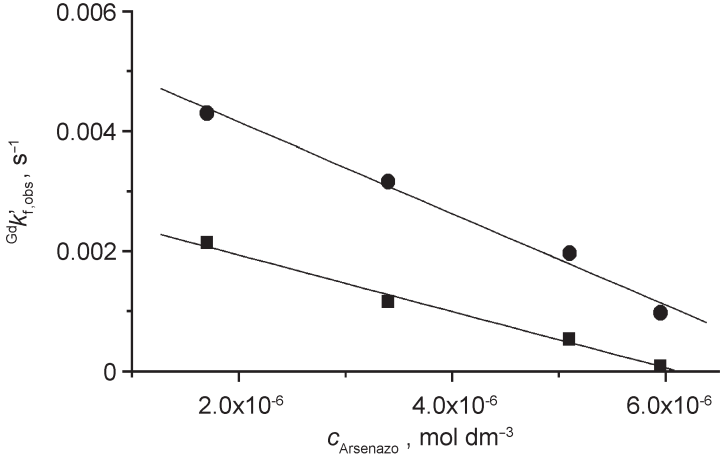

FIG. 7

Examples of the dependence of the pseudo-first order rate constant ${}^{Gd}k'_{f,obs}$ for the formation of $[Gd(Hdo3ap)]^-$/$[Gd(do3ap)]^{2-}$ complexes on the concentration of Arsenazo III and on the solution pH (■ pH 5.93; ● pH 6.30)

$$^{Gd}k_{f,obs} = {}^{Gd}k_{OH}[OH^-] + {}^{Gd}k_{H2O} \quad (14)$$

The calculated parameters are $^{Gd}k_{OH} = (9.0 \pm 0.4) \times 10^4$ l mol^{-1} s^{-1} and $^{Gd}k_{H2O} = (2.26 \pm 0.33) \times 10^{-3}$ s^{-1}. The reaction step characterized by the rate constant $^{Gd}k_{H2O}$ is much slower, representing the transformation of a reaction intermediate to the final product without an assistance of the hydroxide ion[32c,62]. The same rate law was found for the Eu^{3+}–H_5do3ap system and the constants of the same magnitude were estimated[33]. Therefore, the following reaction mechanism can be proposed for the formation of the $[Gd(do3ap)]^{2-}$ complex (Scheme 3; see also Scheme 2 for tentative structures of the intermediates).

The present measurements confirm the commonly accepted fact that cyclen derivatives bind lanthanide(III) ions by a two-step mechanism. The intermediate formed in the first step is double-protonated at the ring nitrogen atoms. Comparing reactivity of ligands with various pendant arms, some changes in reactivity can be observed. Substitution of acetic pendant arms by phosphonic acid ones leads to a decrease in the reactivity because of the bulkiness of the phosphonate groups and/or due to a higher basicity of the ring nitrogen atoms (H_4dota vs H_8dotp, see Tables VIII and IX). The newly synthesized mixed ligand H_5do3ap shows a reactivity between the homosubstituted macrocyclic ligands H_4dota and H_8dotp. With regard to the formation kinetics, H_4dota does not discriminate between the light and medium lanthanides (Ce^{3+} vs Gd^{3+}), in contrast to the heterosubstituted

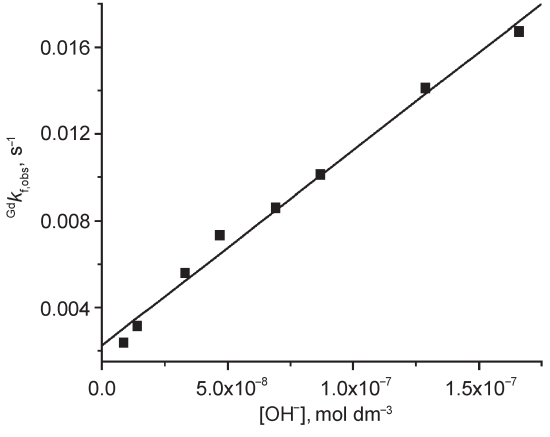

FIG. 8

Dependence of observed pseudo-first order rate constant $^{Gd}k_{f,obs}$ on $[OH^-]$ for formation of $[Gd(Hdo3ap)]^-$/$[Gd(do3ap)]^{2-}$ complexes

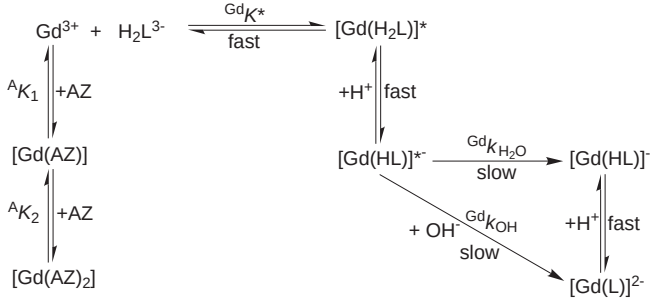

SCHEME 3

Proposed reaction mechanism for the formation of $[Gd(HL)]^-/[Gd(L)]^{2-}$ (L = do3ap^{5-}; Chart 1) complexes

ligand H_5do3ap (see k_{OH} in Table VIII). The stability constant (log *K**) of the kinetic intermediate (Table VIII) for H_4dota is higher than that for H_5do3ap as a possible consequence of the different number of protons in the species.

TABLE IX

Comparison of experimental data for formation and dissociation reactions of Gd^{3+} complexes with H_3do3a, H_4dota, H_8dotp and H_5do3ap[a]

Ligand	Formation[b,c]		Dissociation[d]	
	k_{obs}, s^{-1}	τ(99%)	k_{obs}, s^{-1}	$\tau_{1/2}$
H_3do3a	0.491	11.0 s	6.97×10^{-4}	16.6 min
H_4dota[e]	0.168	27.5 s	8.4×10^{-8}	95.5 h
H_5do3ap	1.49×10^{-3}	0.86 h	2.44×10^{-5}	7.9 h
H_8dotp	1.19×10^{-4}	10.7 h	9.03×10^{-6}	21.3 h

[a] On basis of the data from Table VIII. [b] $c_L \geq 10c_M$ or $c_M \geq 10c_L$ (pseudo-first order conditions). [c] pH 6.0, 25 °C. [d] pH 2.0, 25 °C. [e] Radiometric measurements using metal ion concentration ~10^{-10}–10^{-9} mol l^{-1} (ref.[52]).

Dissociation Kinetics

To determine kinetic inertness of the lanthanide(III) complexes, the acid-assisted decomplexation was performed. Generally, the rate of dissociation of the complexes is given as Eq. (*15*).

$$-\frac{\mathrm{d[complex]}}{\mathrm{d}t} = {}^{\mathrm{Ln}}k_{\mathrm{f,obs}}[\mathrm{complex}]_{\mathrm{tot}} \qquad (15)$$

In the literature, the mechanism of dissociation of H_4dota lanthanide(III) complexes has been established[51]. In our case, there is one extra proton attached to phosphonate and, in the pH region employed, there is no $[Ln(do3ap)]^{2-}$ species present in the mixture (Fig. 4D). Therefore, compared with the H_4dota complexes, our systems are formally shifted by one proton (Scheme 4).

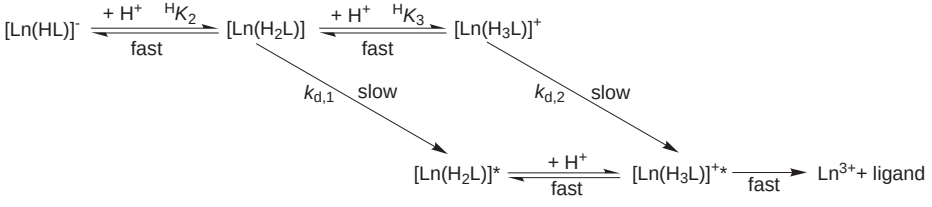

SCHEME 4
Proposed reaction mechanism of acid-assisted dissociation of lanthanide(III) complexes with H_5do3ap (Chart 1)

According to the distribution diagram (Fig. 4D), and taking into account the higher acidity of the solutions used in decomplexation experiments, the mass balance given in Eq. (*16*) can be assumed.

$$[\text{complex}]_{\text{tot}} = [Ln(HL)]^{-} + [Ln(H_2L)] + [Ln(H_3L)]^{+} \qquad (16)$$

The protonation constants of all the species can be written as Eqs (*17*)–(*19*).

$${}^{H}K_1 = \frac{[Ln(HL)]}{[Ln(L)][H^+]} \qquad (17)$$

$${}^{H}K_2 = \frac{[Ln(H_2L)]}{[Ln(HL)][H^+]} \qquad (18)$$

$${}^{H}K_3 = \frac{[Ln(H_3L)]}{[Ln(H_2L)][H^+]} \qquad (19)$$

It is obvious that $\beta_{1Ln} = {}^{H}K_1$, $\beta_{2Ln} = {}^{H}K_1{}^{H}K_2$ and $\beta_{3Ln} = {}^{H}K_1{}^{H}K_2{}^{H}K_3$ (for log β_{1Ln} and log β_{2Ln}, see Table VII). In the case presented in Scheme 4, the dependence of ${}^{Ln}k_{d,obs}$ on $[H^+]$ can be written as Eq. (*20*).

$$ {}^{Ln}k_{f,obs} = \frac{k_{d,1}\,{}^{H}K_2[H^+] + k_{d,2}\,{}^{H}K_2\,{}^{H}K_3[H^+]^2}{1 + {}^{H}K_2[H^+] + {}^{H}K_2\,{}^{H}K_3[H^+]^2} \qquad (20) $$

From Scheme 4, one can suggest that $k_{d,1} << k_{d,2}$. Furthermore, $1 << {}^{H}K_2[H^+] + {}^{H}K_2{}^{H}K_3[H^+]^2$ (cf. the data in Table VII) and, therefore, Eq. (*20*) can be simplified in the following way (Eq. (*21*)).

$$ {}^{Ln}k_{f,obs} \approx \frac{k_{d,2}\,{}^{H}K_2\,{}^{H}K_3[H^+]^2}{{}^{H}K_2[H^+] + {}^{H}K_2\,{}^{H}K_3[H^+]^2} = \frac{k_{d,2}\,{}^{H}K_3[H^+]}{1 + {}^{H}K_3[H^+]} \qquad (21) $$

When ${}^{H}K_3$ is very low, it can be neglected in the denominator and Eq. (*21*) can be rewritten as Eq. (*22*).

$$ {}^{Ln}k_{f,obs} = \frac{k_{d,2}\,{}^{H}K_3[H^+]}{1 + {}^{H}K_3[H^+]} \approx k_{d,2}\,{}^{H}K_3[H^+] = k_{H1}[H^+] \qquad (22) $$

The kinetics of the acid-assisted decomplexation of $[Ln(do3ap)]^{2-}$ complexes were studied in the region 0.01–3.0 M $HClO_4$. The dependence of the pseudo-first order rate constants ${}^{Ln}k_{d,obs}$ on $[H^+]$ is presented in Fig. 9. For Ce^{3+}, this dependence is strictly linear and, therefore, the data were fitted by most simplified Eq. (*22*). However, in the case of Gd^{3+}, some non-

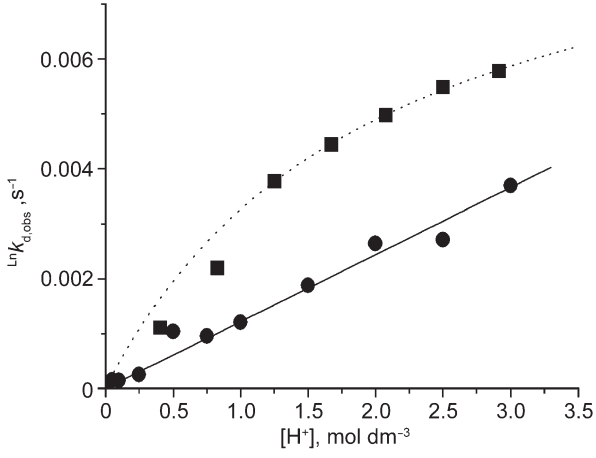

FIG. 9
Dependence of the pseudo-first order rate constant ${}^{Ln}k_{d,obs}$ of the acid-assisted dissociation of complexes $[Ln(do3ap)]^{2-}$ on $[H^+]$. The experimental points were fitted using Eq. (*22*) for Ce^{3+} (●) and by Eq. (*21*) for Gd^{3+} (■)

linearity occurs and the dotted line in Fig. 9 represents a fit according to Eq. (*21*). The same effect was observed for the study of dissociation kinetics of cerium(III)/europium(III)–H_8dotp systems[63].

The linear fit according to Eq. (*22*) for the Ce^{3+} complex gives the values of $k_{H1} = (1.22 \pm 0.04) \times 10^{-3}$ l mol^{-1} s^{-1}. For the non-linear fitting for the Gd^{3+} complex (Eq. (*21*)), the best fit gives $k_{d,2} = (5.8 \pm 0.1) \times 10^{-2}$ s^{-1} and $^{H}K_3 = 0.048 \pm 0.001$ l mol^{-1} consequently leading to the term $k_{H1} = k_{d,2}{}^{H}K_3 = (2.78 \pm 0.07) \times 10^{-3}$ l mol^{-1} s^{-1} (in this way, it can be compared with the previous model used for Ce^{3+}). These results are in accordance with those obtained for the yttrium(III) complex of H_5do3ap, where Eq. (*21*) gives the values $k_{d,2} = 7.00 \times 10^{-3}$ s^{-1}, $^{H}K_3 = 0.192$ l mol^{-1} and $k_{d,2}{}^{H}K_3 = 1.34 \times 10^{-3}$ l mol^{-1} s^{-1} (ref.[34]).

Comparing the results for other Ce^{3+} chelates (Table VIII), it can be seen that the addition of the next pendant group (e.g., acetate or phosphonate) as well as substitution of acetates by phosphonates lead to increased kinetic inertness of such a complex in acidic medium. As expected, the complex of a ligand with a lower denticity (H_3do3a) is less inert than complexes of the other ligands. However, the most stable Gd^{3+} complex of tetrasubstituted cyclen derivatives is the complex with H_4dota. In this case, the inertness of the complex with unsymmetrical ligand H_5do3ap is lower than that for symmetrical ligands (H_4dota, H_8dotp).

CONCLUSIONS

The crystal structure of H_5do3ap confirmed that, in the solid state, the ligand has protons bound to the nitrogen atom close to the phosphonate group and to the trans nitrogen atom. The overall basicity of the ligand is high due to the high value of protonation constant corresponding to removal of the last proton. Successive protonation of ligands leads to several reorganizations of proton binding sites. H_5do3ap has the same arrangement of protons in solution and in the solid state. Stability constants for lanthanide(III) ions are larger than those for H_4dota. Diprotonated species could not be involved in the chemical model describing the “out-of-cell” titrations. Instead, triprotonated species (as equivalents of the transient thermodynamic $[Ln(H_2dota)]^{*+}$ species) had to be considered in the chemical model. The $[Ln(H_3do3ap)]^{+}$ species are probably protonated at two ring nitrogen atoms and the phosphonate group. Similar complexes of the same stoichiometry are assumed to be kinetic intermediates in the complexation of the metal ions by H_5do3ap. The mechanism of formation of the lanthanide(III) complexes follows the generally accepted reaction pathway

with intermediate complexes diprotonated at ring nitrogen atoms. Complexation of the metal ions with H_5do3ap is slower than for the H_4dota complexes under similar conditions. The complexes of H_5do3ap are reasonably inert against acid-assisted decomplexation. Altogether, lanthanide(III) complexes of monophosphorus acid ligands similar to H_5do3ap seem to be suitable for their utilization in medicine.

We thank Ms M. Malíková for help with titration experiments. We also thank Mr J. Rudovský and Dr I. Tišlerová for NMR measurements and Dr I. Císařová for X-ray data collection. The work was supported by the Grant Agency of the Czech Republic (project No. 203/03/0168). The research was performed in the frame of COST D18, NoE EMIL and DiMI European projects.

REFERENCES AND NOTES

1. a) *The Chemistry of Contrast Agents in Medical Magnetic Resonance Imaging* (A. E. Merbach and É. Tóth, Eds). Wiley, Chichester 2001; b) *Top. Curr. Chem.* **2002**, Vol. *221*; c) Caravan P., Ellison J. J., Mc Murry T. J., Laufer R. B.: *Chem. Rev.* **1999**, *99*, 2293.
2. a) Li W. P., Meyer L. A., Anderson C. J.: *Top. Curr. Chem.* **2005**, *252*, 179; b) Liu S.: *Chem. Soc. Rev.* **2004**, *33*, 445; c) *Handbook of Radiopharmaceuticals. Radiochemistry and Applications* (M. J. Welch and C. S. Redvanly, Eds). Wiley, Chichester 2003; d) Liu S., Edwards D. S.: *Bioconjugate Chem.* **2001**, *12*, 7.
3. a) Zalutsky M. R., Lewis J. S. in: *Handbook of Radiopharmaceuticals. Radiochemistry and Applications* (M. J. Welch and C. S. Redvanly, Eds), p. 685–714. Wiley, Chichester 2003; b) Goldenberg D. M.: *J. Nucl. Med.* **2002**, *43*, 693; c) Juweid M. E.: *J. Nucl. Med.* **2002**, *43*, 1507.
4. a) Fichna J., Janecka A.: *Bioconjugate Chem.* **2003**, *14*, 3; b) de Jong M., Kwekkeboom D. J., Valkema R., Krenning E. P.: *Eur. J. Nucl. Med.* **2003**, *30*, 463; c) Knight L. C. in: *Handbook of Radiopharmaceuticals. Radiochemistry and Applications* (M. J. Welch and C. S. Redvanly, Eds), p. 643–684. Wiley, Chichester 2003.
5. McMurry T. J., Pippin C. G., Wu C., Deal K. A., Brechbiel M. W., Mirzadeh S., Gansow O. A.: *J. Med. Chem.* **1998**, *41*, 3546.
6. Meyer M., Dahaoui-Gindrey V., Lecomte C., Guilard R.: *Coord. Chem. Rev.* **1998**, *178–180*, 1313.
7. Lukeš I., Kotek J., Vojtíšek P., Hermann P.: *Coord. Chem. Rev.* **2001**, *216–217*, 287.
8. Sherry A. D.: *J. Alloys Compd.* **1997**, *249*, 153.
9. Belskii I., Polikarpov Yu. M., Kabachnik M. I.: *Usp. Khim.* **1992**, *61*, 415.
10. Kabachnik M. I., Medved T. Ya., Polikarpov Yu. M., Shcherbakov B. K., Belskii F. I., Matrosov E. I., Pasechnik M. I.: *Izv. Akad. Nauk SSSR, Ser. Khim.* **1984**, 835.
11. a) Sherry A. D., Ren J., Huskens J., Brücher E., Tóth E., Geraldes C. F. C. G., Castro M. M. C. A., Cacheris W. P.: *Inorg. Chem.* **1996**, *35*, 4604; b) Delgado R., Siegfried L. C., Kaden T. A.: *Helv. Chim. Acta* **1990**, *73*, 140; c) Kabachnik I. M., Medved T. Ya., Belskii F. I., Pisareva S. A.: *Izv. Akad. Nauk SSSR, Ser. Khim.* **1984**, 844.
12. Pisareva S. A., Belskii F. I., Medved T. Ya, Kabachnik M. I.: *Izv. Akad. Nauk SSSR, Ser. Khim.* **1987**, 413.
13. Burai L. Király R., Lázár I., Brücher E.: *Eur. J. Inorg. Chem.* **2001**, 813.

14. Sun X., Wuest M., Kovacs Z., Sherry A. D., Motekaitis R., Wang Z., Martell A. E., Welch M. J., Anderson C. J.: *J. Biol. Inorg. Chem.* **2003**, *8*, 217.
15. a) Lázár I., Sherry A. D., Ramasamy R., Brücher E., Király R.: *Inorg. Chem.* **1991**, *30*, 5016; b) Bazakas K., Lukeš I.: *J. Chem. Soc., Dalton Trans.* **1995**, 1133; c) Rohovec J., Kývala M., Vojtíšek P., Hermann P., Lukeš I.: *Eur. J. Inorg. Chem.* **2000**, 195.
16. Pulukkody K., Norman T. J., Parker D., Royle L., Broan C. J.: *J. Chem. Soc., Perkin Trans. 2* **1993**, 605.
17. Lubal P., Kývala M., Hermann P., Holubová J., Rohovec J., Havel J., Lukeš I.: *Polyhedron* **2001**, *20*, 7.
18. Parker D., Dickins R. S., Puschmann H., Crossland C., Howard J. A. K.: *Chem. Rev.* **2002**, *102*, 1977.
19. a) Lebdušková P., Kotek J., Hermann P., Elst L. V., Muller R. N., Lukeš I., Peters J. A.: *Bioconjugate Chem.* **2004**, *15*, 881; b) Kotek J., Lebdušková P., Hermann P., Elst L. V., Muller R. N., Maschmeyer T., Lukeš I., Peters J. A.: *Chem. Eur. J.* **2003**, *9*, 5899.
20. a) Rudovský J., Cígler P., Kotek J., Hermann P., Vojtíšek P., Lukeš I., Peters J. A., Elst L. V., Muller R. N.: *Chem. Eur. J.* **2005**, *11*, 2373; b) Vojtíšek P., Cígler P., Kotek J., Rudovský J., Hermann P., Lukeš I.: *Inorg. Chem.* **2005**, *44*, 5591.
21. Rudovský J., Kotek J., Hermann P., Lukeš I., Mainero V., Aime S.: *Org. Biomol. Chem.* **2005**, *3*, 112.
22. Rudovský J., Hermann P., Botta M., Aime S., Lukeš I.: *Chem. Commun.* **2005**, 2390.
23. All lanthanide(III) complexes of H_5do3ap discussed in this text contain in solution one water molecule bound directly to the central metal ion. As the water molecule is not relevant for most of the following text, it is omitted in all formulas.
24. a) Bornais J., Brownstein S.: *J. Magn. Reson.* **1978**, *29*, 207; b) van Geet A. L.: *Anal. Chem.* **1970**, *42*, 679.
25. a) Otwinovski Z. , Minor W.: *HKL Denzo and Scalepack Program Package*. Nonius BV, Delft 1997; b) Otwinovski Z., Minor W.: *Methods Enzymol.* **1997**, *276*, 307.
26. Altomare A., Burla M. C., Camalli M., Cascarano G., Giacovazzo C., Guagliardi A., Polidori G.: *J. Appl. Crystallogr.* **1994**, *27*, 435.
27. Sheldrick G. M.: *SHELXL97*. Program for Crystal Structure Refinement from Diffraction Data. University of Göttingen, Göttingen 1997.
28. a) Kývala M., Lukeš I.: *International Conference Chemometrics '95, Pardubice, Czech Republic*, p. 63; full version of "OPIUM" is available on http://www.natur.cuni.cz/~kyvala/opium.html; b) Kývala M., Lubal P., Lukeš I.: Presented at *IXth Spanish–Italian and Mediterranean Congress on Thermodynamics of Metal Complexes, Girona, Spain 1998*.
29. Martell A. E., Smith R. M.: *Critical Stability Constants*, Vols 1–6. Plenum Press, New York 1974–1989; *NIST Standard Reference Database 46* (*Critically Selected Stability Constants of Metal Complexes*), Version 7.0, 2003.
30. Baes C. F., Jr., Mesmer R. E.: *The Hydrolysis of Cations*. Wiley, New York 1976.
31. Alner D. J., Greczek J. J., Smeeth A. G.: *J. Chem. Soc. A* **1967**, 1205.
32. a) Cai H.-Z., Kaden T. A.: *Helv. Chim. Acta* **1994**, *77*, 383; b) Kumar K., Chang C. A., Tweedle M. F.: *Inorg. Chem.* **1993**, *32*, 587; c) Kumar K., Tweedle M. F.: *Inorg. Chem.* **1993**, *32*, 4193.
33. a) Táborský P., Svobodová I., Hnatejko Z., Lubal P., Lis S., Försterová M., Hermann P., Lukeš I., Havel J.: *J. Fluorescence* **2005**, *15*, 507; b) Táborský P., Svobodová I., Lubal P., Hnatejko Z., Piskula Z., Lis S., Havel J., Hermann P., Lukeš I.: Unpublished results.

34. Svobodová I., Försterová M., Táborský P., Lubal P., Kotek J., Hermann P., Lukeš I.: Unpublished results.
35. Kotek J., Hermann P., Lukeš I.: Unpublished results.
36. Lázár I., Hrncir D. C., Kim W.-D., Kiefer G. E., Sherry A. D.: *Inorg. Chem.* **1992**, *31*, 4422.
37. Bianchi A., Calabi L., Giorgi C., Losi P., Palma M., Paoli P., Rossi P., Valtancoli B., Virtuani M.: *J. Chem. Soc., Dalton Trans.* **2000**, 697.
38. a) Popov A., Ronkkomaki H., Popov K., Lajunen L. H. J., Vendilo A.: *Inorg. Chim. Acta* **2003**, 353, 1; b) Popov K., Ronkkomaki H., Lajunen L. H. J.: *Pure Appl. Chem.* **2001**, *73*, 1641; c) Popov K., Niskanen E., Ronkkomaki H., Lajunen H. J.: *New J. Chem.* **1999**, *23*, 1209.
39. Kotek J., Vojtíšek P., Císařová I., Hermann P., Jurečka P., Rohovec J., Lukeš I.: *Collect. Czech. Chem. Commun.* **2000**, *65*, 1289.
40. Delgado R., Costa J., Guerra K. P., Lima L. M. P.: *Pure Appl. Chem.* **2005**, *77*, 569.
41. Kiss T., Lázár I. in: *Aminophosphonic and Aminophosphinic Acids. Chemistry and Biological Activity* (V. P. Kukhar and H. R. Hudson, Eds), Chap. IX, p. 285–326. Wiley, Chichester 2000.
42. Chaves S., Delgado R., Frausto Da Silva J. J. R.: *Talanta* **1992**, *39*, 249.
43. Burai L., Fábián I., Király R., Szilágyi E., Brücher E.: *J. Chem. Soc., Dalton Trans.* **1998**, 243.
44. Moreau J., Guillon E., Pierrard J.-C., Rimbault J., Port M., Aplincourt M.: *Chem. Eur. J.* **2004**, *10*, 5218.
45. Burai L., Ren J., Kovacs Z., Brücher E., Sherry A. D.: *Inorg. Chem.* **1998**, *37*, 69.
46. Appleton T. G., Hall J. R., Harris A. D., Kimlin M. A., Mc Mahon I. J.: *Aust. J. Chem.* **1984**, *37*, 1833.
47. Geraldes C. F. G. C., Sherry A. D., Cacheris W. P.: *Inorg. Chem.* **1989**, *28*, 3336.
48. Guerra K. P., Delgado R., Lima L. M. P., Drew M. G. B., Félix V.: *Dalton Trans.* **2004**, 1812.
49. Cacheris W. P., Nickle S. K., Sherry A. D.: *Inorg. Chem.* **1987**, *26*, 958.
50. Tóth É., Brücher E., Lázár I., Tóth I.: *Inorg. Chem.* **1994**, *33*, 4070.
51. Wu S.-L., Horrocks W. deW., Jr.: *Inorg. Chem.* **1995**, *34*, 3724.
52. Wang X., Tianzhu J., Comblin V., Mut A. L., Merciny E., Desreux J. F.: *Inorg. Chem.* **1992**, *31*, 1095.
53. Nash K. L., Rogers R. D., Ferraro J., Zhang J.: *Inorg. Chim. Acta* **1998**, *269*, 211.
54. Szilágyi E., Tóth É, Brücher E., Merbach A. E.: *J. Chem. Soc., Dalton Trans.* **1999**, 2481.
55. Kotek J., Císařová I., Hermann P., Lukeš I., Rohovec J.: *Inorg. Chim. Acta* **2001**, *317*, 324.
56. Kotek J., Vojtíšek P., Císařová I., Hermann P., Lukeš I.: *Collect. Czech. Chem. Commun.* **2001**, *66*, 363.
57. Kotek J., Lubal P., Hermann P., Císařová I., Lukeš I., Godula T., Svobodová I., Táborský P., Havel J.: *Chem. Eur. J.* **2003**, *9*, 233.
58. Brücher E., Laurency G., Makra Z.: *Inorg. Chim. Acta* **1987**, *139*, 141.
59. Brücher E., Sherry A. D.: *Inorg. Chem.* **1990**, *29*, 1555.
60. Szilágyi E., Tóth É., Kovács Z., Platzek J., Radüchel B., Brücher E.: *Inorg. Chim. Acta* **2000**, *298*, 226.
61. Vojtíšek P., Rohovec J.: Private communication.
62. Jang Y.-H., Blanco M., Dasgupta S., Keire D. A., Shively J. E., Goddard W. A.: *J. Am. Chem. Soc.* **1999**, *121*, 6142.
63. Chang C. A., Liu Y.-L.: *J. Chin. Chem. Soc.* **2000**, *47*, 1001.

64. Svobodová I., Piskula Z., Lubal P.: Unpublished results.
65. Reddy K. B., Cao S., Orr E. C., Fabián I., van Eldik R., Eyring E. M.: *J. Chem. Soc., Dalton Trans.* **1994**, 2497.
66. Shi Y., Ji Q., Eyring E. M., van Eldik R.: *J. Chem. Soc., Dalton Trans.* **1996**, 2127.
67. a) Lu Y.-W., Laurent G., Pereira H.: *Talanta* **2004**, *62*, 959; b) Hosten E., Rohwer H.: *Anal. Chim. Acta* **1997**, *345*, 227; c) Rohwer H., Hosten E.: *Anal. Chim. Acta* **1997**, *339*, 271; d) Rohwer H., Collier N., Hosten E.: *Anal. Chim. Acta* **1995**, *314*, 219.
68. Iranzo O., Kovalevsky A. Y., Morrow J. R., Richard J. P.: *J. Am. Chem. Soc.* **2003**, *125*, 1988.